

# Hybrid quantum logic and a test of Bell's inequality using two different atomic species

C. J. Ballance, V. M. Schäfer, J. P. Home, D. J. Szwer, S. C. Webster, D. T. C. Allcock, N. M. Linke, T. P. Harty, D. P. L. Aude Craik, D. N. Stacey, A. M. Steane and D. M. Lucas  
*Department of Physics, University of Oxford, Clarendon Laboratory, Parks Road, Oxford OX1 3PU, U.K.*  
(Dated: v2.4, 15 May 2015)

Entanglement is one of the most fundamental properties of quantum mechanics, and is the key resource for quantum information processing. Bipartite entangled states of identical particles have been generated and studied in several experiments, and post-selected entangled states involving pairs of photons, or single photons and single atoms, have also been produced. Here, we deterministically generate a “hybrid” entangled state of two different species of trapped-ion qubit, perform full tomography of the state produced, and make the first test of Bell's inequality with non-identical atoms. We use a laser-driven two-qubit quantum logic gate, whose mechanism is insensitive to the qubits' energy splittings, to produce a maximally-entangled state of one  $^{40}\text{Ca}^+$  qubit and one  $^{43}\text{Ca}^+$  qubit, held in the same ion trap, with 99.8(5)% fidelity. We make a test of Bell's inequality for this novel entangled state, and find that it is violated by  $15\sigma$ . Mixed-species quantum logic is an essential technique for the construction of a quantum computer based on trapped ions, as it allows protection of memory qubits while other qubits undergo logic operations, or are used as photonic interfaces to other processing units.

For Schrödinger, entanglement was “the characteristic trait of quantum mechanics” [1] and it has been at the heart of debates about the foundations of quantum mechanics since the framing of the Einstein-Podolsky-Rosen paradox [2]. The theoretical work of Bell [3], and of Clauser *et al.* [4], established an experimental test which could be used to rule out local hidden-variable theories on the basis of correlations between measured properties of entangled particles, and numerous experiments, starting with that of Freedman and Clauser, have confirmed the predictions of quantum mechanics [5–9]. Tests of Bell's inequality with trapped ions were the first to close the so-called “detector loophole”; hitherto these have exclusively been carried out with identical atoms [7, 10, 11]. The entanglement explored in tests of Bell's inequality is typically an entanglement between distinguishable particles, in the strict quantum mechanical sense, but when the particles are identical in their internal structure and state, they are distinguishable only through their spatial localization. By employing different isotopes, our experiments involve entities that are also distinguishable by many internal properties, such as baryon number, mass,

spin, resonant frequencies, and so on.

Apart from its intrinsic interest, entanglement is a central resource for quantum information applications, such as quantum cryptography [12] and quantum computing [13]. Trapped atomic ions are one of the most promising technologies for the implementation of quantum computation; several demonstrations of simple multi-qubit algorithms have been made [14] and the elementary set of quantum logic operations has recently been demonstrated with the precision required for the implementation of fault-tolerant techniques [15, 16]. Scaling up trapped-ion systems to the large numbers of qubits required for useful quantum information processing will almost certainly require the use of more than one species of ion, both for the purpose of sympathetic laser-cooling [17–19] and for providing robust memory qubits: the best memory qubits reside in hyperfine ground states [15, 20], which have essentially infinite lifetimes against spontaneous decay, but are vulnerable to the scattering of a single photon of resonant laser light. In a complex, multi-zone, ion trap processor it will be difficult to shield the memory qubits sufficiently well from resonant laser beams, hence it will be useful to employ different species of ion, for example, as “memory” and “logic” qubits, which in turn requires a two-qubit quantum logic gate capable of mapping quantum states from one species to another.

In the present work, we entangle qubits stored in two different isotopes of calcium. The  $^{40}\text{Ca}^+$  qubit is stored in the Zeeman-split ground level,  $(|\downarrow\rangle, |\uparrow\rangle) = (4S_{1/2}^{-1/2}, 4S_{1/2}^{+1/2})$ , and the  $^{43}\text{Ca}^+$  qubit is stored in the hyperfine ground states  $(|\downarrow\rangle, |\uparrow\rangle) = (4S_{1/2}^{4,+4}, 4S_{1/2}^{3,+3})$  (figure 1). The qubit energy splittings differ by some three orders of magnitude ( $f_{\uparrow} \approx 5.4$  MHz,  $f_{\downarrow} \approx 3.2$  GHz), but they may nevertheless be efficiently coupled via the two-qubit gate mechanism of Leibfried *et al.* [21], in which the “travelling standing wave” from a pair of far-detuned laser beams exerts a qubit-state-dependent force on the ions whose magnitude  $F$  is largely independent of the qubit frequency. The force originates from a spatially-varying light shift, oscillates at the difference frequency  $\delta$  between the two beams and, when  $\delta = f_z + \delta_g$  is set close to the resonant frequency  $f_z$  of a normal mode of motion of the two-ion crystal, a two-qubit phase gate may be implemented by applying the force for a time  $t_g = 1/\delta_g$ .

An important difference in the gate mechanism compared with the case of identical ions is that the forces

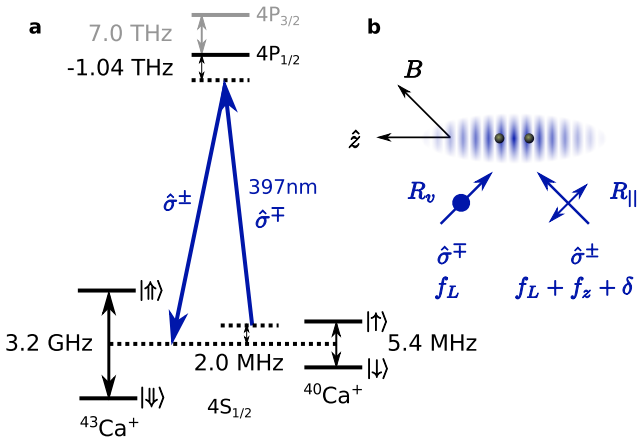


FIG. 1: (a) Qubit states and Raman transitions in  $^{43}\text{Ca}^+$  and  $^{40}\text{Ca}^+$ . The two Raman beams have a mean detuning of  $\Delta = -1.04$  THz from the  $4S_{1/2}$ - $4P_{1/2}$  (397 nm) transition, and a difference frequency of  $\delta = f_z + \delta_g \approx 2$  MHz. (b) Raman beam geometry. The two beams are aligned to set the lattice k-vector parallel to the trap axis  $z$ . The beams have a waist radius of  $w = 27 \mu\text{m}$ , a power of  $\approx 5$  mW each, and orthogonal linear polarizations as indicated. The quantization axis is set by a magnetic field  $B \approx 2$  G.

on corresponding qubit states differ ( $F_{\uparrow} \neq F_{\downarrow}$  and  $F_{\downarrow} \neq F_{\uparrow}$ ) so that, in general, the four possible qubit states ( $\uparrow\uparrow, \uparrow\downarrow, \downarrow\uparrow, \downarrow\downarrow$ ) each acquire different phases. We choose to implement the gate operation in two halves, each of duration  $t_g = 1/\delta_g$ , separated by spin-flip operations ( $\pi$ -pulses) on the qubits (figure 2a). This symmetrizes the gate operation such that the relative phases acquired by the four states are  $(0, \Phi, \Phi, 0)$ . By setting the laser power (i.e., effective Rabi frequency) and gate detuning  $\delta_g$  appropriately, and enclosing the gate operation in a Ramsey interferometer (two pairs of  $\pi/2$ -pulses), we can generate the maximally-entangled Bell state  $(|\downarrow\downarrow\rangle + |\uparrow\uparrow\rangle)/\sqrt{2}$  from the initial state  $|\downarrow\downarrow\rangle$ . The  $\pi$ -pulses also protect the qubits against dephasing due to slow ( $\gg t_g$ ) variations in magnetic fields.

In our experiment, we implement the gate using the in-phase axial motional mode (at  $f_z = 2.00$  MHz) of a linear Paul trap [22], with the ion separation ( $3.5 \mu\text{m}$ ) equal to a half-integer number of standing wavelengths, thus exciting the motion maximally for the  $|\uparrow\downarrow\rangle$  and  $|\downarrow\uparrow\rangle$  states. The Lamb-Dicke parameters for the two different mass isotopes are  $\eta_{\downarrow} = 0.121$  and  $\eta_{\uparrow} = 0.126$ . After initial Doppler cooling, both axial modes are cooled close to their ground states ( $\bar{n} < 0.1$ ) by Raman sideband cooling applied to the  $^{40}\text{Ca}^+$  ion (which sympathetically cools the  $^{43}\text{Ca}^+$  ion). Both qubits are initialized by optical pumping, after which we apply the gate sequence shown in figure 2a, using a gate duration  $2t_g = 27.4 \mu\text{s}$ . Single-qubit  $\pi/2$ - and  $\pi$ -pulses, for the spin-echo and tomography operations, are applied using co-propagating Raman beams (for  $^{40}\text{Ca}^+$ ) and microwaves (for  $^{43}\text{Ca}^+$ ).

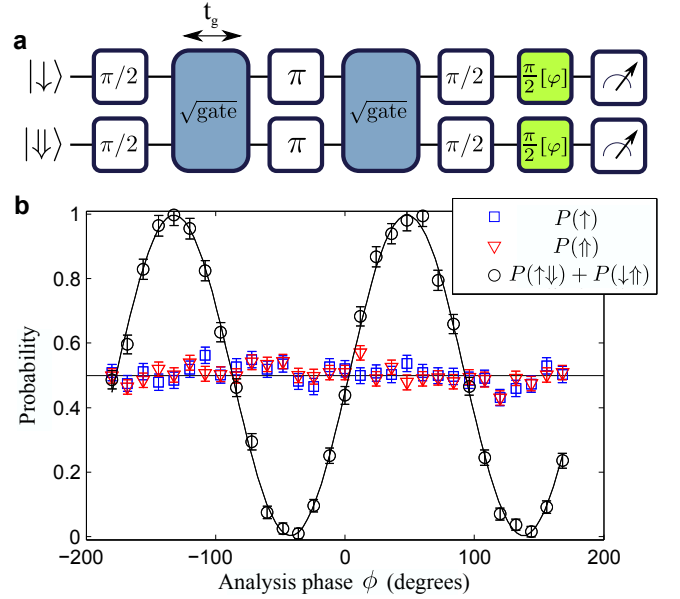


FIG. 2: (a) Gate operation sequence. The final “analysis”  $\pi/2$ -pulses (green) are optional; by scanning their phase  $\phi$  we can diagnose the state produced by the gate. (b) Qubit populations and parity signal after correcting for readout errors. The individual qubit populations are measured without analysis pulses, and are consistent with  $\frac{1}{2}$ , as expected for the Bell state  $(|\downarrow\downarrow\rangle + |\uparrow\uparrow\rangle)/\sqrt{2}$ . With the analysis pulses, the parity signal  $P(\uparrow\downarrow) + P(\downarrow\uparrow)$ , i.e. the probability of the two qubits being in opposite states, should oscillate between 0 and 1 as  $\sin(2\phi)$  for a perfect Bell state. From these measurements we infer a Bell state fidelity of 99.8(5)%. The error bars show  $1\sigma$  statistical errors.

The ordering of the ion pair in the trap was kept constant over the time taken to acquire the full data set, to guard against systematic effects associated with ion position (see Methods). We implement individual qubit readout by simultaneously state-selectively shelving both ions to the  $3D_{5/2}$  level, then detecting the ions’ fluorescence sequentially in two photomultiplier counting periods (see Methods).

From the contrast of the parity fringes shown in figure 2, and a measurement of the qubit populations before the analysis pulses, we estimate the fidelity of the Bell state produced by the gate to be  $\mathcal{F} = 99.8(5)\%$ , where the error is dominated by statistical uncertainty. Known contributions to the gate error are significantly smaller [16], for example the photon scattering error at the  $\Delta = -1.04$  THz Raman detuning used is estimated to be  $\approx 0.1\%$ . Since the two qubits may be rotated independently by addressing them in frequency space, we can also perform full tomography of the entangled state and extract the density matrix (figure 3); the density matrix is consistent with that for the desired Bell state, to within the systematic errors from the imperfect tomography pulses, and gives a separate estimate of the fidelity  $\mathcal{F} = 99(1)\%$ .

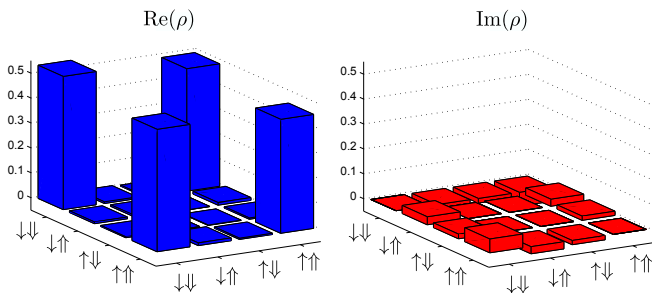


FIG. 3: Density matrix of the Bell state (real and imaginary parts) after correcting for qubit readout errors. This was measured by rotating each qubit independently to perform full quantum state tomography. We used a maximum likelihood method to find the density matrix that best represents the experimental data. This gives a separate estimate of the gate fidelity, 99(1)%.

$\theta_a$ ( $^{40}\text{Ca}^+$ )	$\pi/4$	$3\pi/4$	$\pi/4$	$3\pi/4$
$\theta_b$ ( $^{43}\text{Ca}^+$ )	$\pi/2$	$\pi/2$	0	0
$E(\theta_a, \theta_b)$	0.565(7)	0.530(7)	0.560(7)	-0.573(8)

TABLE I: Bell/CHSH inequality test results, using the mixed-species entangled state. The qubits are independently rotated through angles  $(\theta_a, \theta'_a) = (\pi/4, 3\pi/4)$  and  $(\theta_b, \theta'_b) = (\pi/2, 0)$ , and for each combination of angles the correlation function  $E(\theta_a, \theta_b)$  is measured, with results shown. ( $E$  is defined as in ref.[10].) The CHSH parameter is given by  $S = |E(\theta_a, \theta_b) + E(\theta'_a, \theta_b)| + |E(\theta_a, \theta'_b) - E(\theta'_a, \theta'_b)| = 2.228(15) > 2$ , thus violating Bell’s inequality for this system of non-identical atoms. The state detection is sufficiently accurate that it is not necessary to make a fair-sampling assumption.

To perform a test of the CHSH version of Bell’s inequality, we follow the gate sequence with further independent single-qubit rotations and measurements. The single qubit rotations have constant phase  $\phi$  but varying rotation angle  $\theta$ . From these measurements we determine the two-particle correlation functions with results shown in table I. As is well known, the maximal CHSH parameter  $S$  allowed by local hidden-variable theories is 2, whereas quantum mechanics allows  $S \leq 2\sqrt{2}$ . In these experiments we do not correct for qubit readout errors, in order to avoid making a fair-sampling assumption. This limits us to a detectable maximum  $S_{\text{max}} = 2.236(7)$ ; our results give  $S = 2.228(15)$ , consistent with  $S_{\text{max}}$  to within the stated uncertainties, and violating the CHSH inequality by  $\approx 15\sigma$ .

The mixed-species quantum logic gate that we have demonstrated has allowed us to create a novel entangled state, leading to the first test of a Bell inequality violation between non-identical atoms. As an application, the two isotopes used here could be employed for scalable quantum computing architectures based on trapped ions; hyperfine qubits in  $^{43}\text{Ca}^+$  at present constitute the best single-qubit memories ( $T_2^* \sim 1$  min) [15], whereas the simpler atomic structure of  $^{40}\text{Ca}^+$  is well suited for use as a

“photonic interconnect” qubit [23]. There are technical advantages to using ions of similar mass for sympathetic cooling and ion transport in multi-zone traps. However, while the relatively small isotope shifts ( $\sim 1$  GHz) allow the convenient use of the same laser systems for manipulation of both species, they may provide insufficient protection of qubits from stray resonant light. Therefore in the long term it may be necessary to use different atomic elements [18]. The gate mechanism employed here is independent of the qubit frequency and thus can also be used to couple qubits stored in different elements, provided that the Raman laser fields exert sufficient force on both qubits.

We note that  $\text{Ca}^+$  and  $\text{Sr}^+$  ions are an attractive choice in this respect: the  $4\text{S}_{1/2}-4\text{P}_{1/2}$  transition in  $\text{Ca}^+$  is separated from the  $4\text{S}_{1/2}-4\text{P}_{3/2}$  transition in  $\text{Sr}^+$  by 20 THz. A Raman laser detuning  $\Delta \approx -8$  THz (comparable to that used in our recent  $^{43}\text{Ca}^+-^{43}\text{Ca}^+$  two-qubit gate experiments [16]) would enable the implementation of a mixed-species logic gate with a photon-scattering error of  $\sim 10^{-4}$ , significantly below the error threshold for fault-tolerant operations [24].

Related experiments have recently also been carried out in the NIST Ion Storage Group [27].

## METHODS

To perform the state readout of each qubit we state-selectively shelve one of the qubit states to the  $3\text{D}_{5/2}$  level, then apply the Doppler cooling lasers. If the ion was not shelved it fluoresces, and this is detected with a photomultiplier.

We simultaneously shelve the two species using a weak 393 nm beam resonant with the  $^{43}\text{Ca}^+ 4\text{S}_{1/2}^{4,+4}-4\text{P}_{3/2}^{5,+5}$  transition, with a 1.94 GHz EOM sideband which drives the  $^{40}\text{Ca}^+ 4\text{S}_{1/2}^{+1/2}-4\text{P}_{3/2}^{+3/2}$  transition. An intense 850 nm beam resonant with the  $^{40}\text{Ca}^+ 3\text{D}_{3/2}-4\text{P}_{3/2}$  transition makes the shelving for this isotope state-selective, through an EIT process involving the two transitions [25]. The  $^{43}\text{Ca}^+$  shelving is state-selective due to the 3.2 GHz splitting between the two qubit states [26]. Both these shelving processes have a maximum theoretical efficiency of  $\approx 90\%$  due to leakage to  $3\text{D}_{3/2}$  (which for  $^{43}\text{Ca}^+$  could be eliminated using a further 850 nm beam if required [26]), leading to readout errors of  $\approx 5\%$  when averaged over both qubit states.

Typical combined state-preparation and readout errors are measured to be  $\epsilon_{\downarrow, \uparrow} = 7.4(3)\%, 7.9(3)\%$  for  $^{40}\text{Ca}^+$  and  $\epsilon_{\downarrow, \uparrow} = 6.5(3)\%, 2.3(3)\%$  for  $^{43}\text{Ca}^+$ . We estimate the systematic errors in determining the state-preparation and readout error to be  $\approx 0.1\%$ , less than the statistical error in these measurements. From independent experiments we estimate the state-preparation error to be  $\approx 0.1\%$ , hence the dominant error we are normalising out is the readout error.

The ion crystal ordering is kept constant over the experiments to control systematic errors. The principal error which would arise if the ion order were not controlled is due to an (undesired) axial magnetic field gradient that causes the magnetic field between the two ions to differ by 1.8 mG. This means that the qubit frequencies for the two possible ion orders differ by  $\approx 5$  kHz, which would lead to errors in single-qubit rotations. The change in qubit frequency allows us to detect the ion order: if it is wrong, we randomly reorder the crystal until the order is correct with a short period of Doppler heating to melt the crystal, followed by a short period of Doppler cooling.

To suppress off-resonant excitation during the entangling gate we shape the gate Rabi frequency with a characteristic time of 1  $\mu$ s; without this pulse-shaping the off-resonant excitation would lead to a gate error of  $\lesssim 5\%$ .

We adjust the polarisation of each Raman beam to null the differential ‘single-beam’ light-shift on the  $^{40}\text{Ca}^+$  qubit. Due to the difference in atomic structure there is a residual light-shift on the  $^{43}\text{Ca}^+$  qubit of  $\approx 0.2\%$  of the light-shift for a purely circularly-polarised beam. This small light-shift does not cause any significant issues in the experiments reported here; if necessary it could be suppressed further by increasing the Raman detuning at the expense of requiring more Raman beam power.

- 
- [1] E. Schrödinger and M. Born, *Mathematical Proceedings of the Cambridge Philosophical Society* **31**, 555 (1935).
- [2] A. Einstein, B. Podolsky, and N. Rosen, *Physical Review A* **47**, 777 (1935).
- [3] J. S. Bell, *Physics* **1**, 195 (1964).
- [4] J. F. Clauser, M. A. Horne, A. Shimony, and R. A. Holt, *Physical Review Letters* **23**, 880 (1969).
- [5] S. J. Freedman and J. F. Clauser, *Physical Review Letters* **28**, 938 (1972).
- [6] A. Aspect, P. Grangier, and G. Roger, *Physical Review Letters* **49**, 91 (1982), ISSN 00319007.
- [7] M. A. Rowe, D. Kielpinski, V. Meyer, C. A. Sackett, W. M. Itano, C. Monroe, and D. J. Wineland, *Nature* **409**, 791 (2001), ISSN 00280836.
- [8] D. Moehring, M. Madsen, B. Blinov, and C. Monroe, *Physical Review Letters* **93**, 2 (2004), ISSN 0031-9007.
- [9] M. Giustina, A. Mech, S. Ramelow, B. Wittmann, J. Kofler, J. Beyer, A. Lita, B. Calkins, T. Gerrits, S. W. Nam, et al., *Nature* **497**, 227 (2013), ISSN 1476-4687.
- [10] D. N. Matsukevich, P. Maunz, D. L. Moehring, S. Olmschenk, and C. Monroe, *Physical Review Letters* **100**, 150404 (2008), ISSN 0031-9007.
- [11] B. P. Lanyon, M. Zwerger, P. Jurcevic, C. Hempel, W. Dür, H. J. Briegel, R. Blatt, and C. F. Roos, *Physical Review Letters* **112** (2014), ISSN 00319007, 1312.4810.
- [12] A. K. Ekert, *Physical Review Letters* **67**, 661 (1991).
- [13] D. Deutsch, *Proceedings of the Royal Society A: Mathematical, Physical and Engineering Sciences* **400**, 97 (1985), ISSN 1364-5021.
- [14] R. Blatt and D. J. Wineland, *Nature* **453**, 1008 (2008), ISSN 1476-4687.
- [15] T. P. Harty, D. T. C. Allcock, C. J. Ballance, L. Guidoni, H. A. Janacek, N. M. Linke, D. N. Stacey, and D. M. Lucas, *Physical Review Letters* **113**, 220501 (2014), ISSN 0031-9007.
- [16] C. J. Ballance, T. P. Harty, N. M. Linke, and D. M. Lucas, arXiv:1406.5473.
- [17] D. J. Wineland, C. Monroe, W. M. Itano, D. Leibfried, B. E. King, and D. M. Meekhof, *Journal Of Research Of The National Institute Of Standards And Technology* **103**, 259 (1998).
- [18] M. D. Barrett, B. DeMarco, T. Schaetz, V. Meyer, D. Leibfried, J. W. Britton, J. Chiaverini, W. M. Itano, B. Jelenković, J. D. Jost, et al., *Physical Review A* **68**, 042302 (2003), ISSN 1050-2947.
- [19] J. P. Home, D. Hanneke, J. D. Jost, J. M. Amini, D. Leibfried, and D. J. Wineland, *Science* **325**, 1227 (2009), ISSN 1095-9203.
- [20] C. E. Langer, R. Ozeri, J. D. Jost, J. Chiaverini, B. DeMarco, A. Ben-Kish, R. B. Blakestad, J. W. Britton, D. B. Hume, W. M. Itano, et al., *Physical Review Letters* **95**, 060502 (2005), ISSN 0031-9007.
- [21] D. Leibfried, B. DeMarco, V. Meyer, D. M. Lucas, M. D. Barrett, J. W. Britton, W. M. Itano, B. Jelenković, C. E. Langer, T. Rosenband, et al., *Nature* **422**, 412 (2003), ISSN 0028-0836.
- [22] C. J. Ballance, Ph.D. thesis, University of Oxford (2014).
- [23] C. Monroe and J. Kim, *Science* **339**, 1164 (2013), ISSN 0036-8075.
- [24] A. G. Fowler, M. Mariantoni, J. M. Martinis, and A. N. Cleland, *Physical Review A* **86**, 032324 (2012), ISSN 1050-2947.
- [25] M. J. McDonnell, J.-p. Stacey, S. C. Webster, J. P. Home, A. Ramos, D. M. Lucas, D. N. Stacey, and A. M. Steane, *Physical Review Letters* **93**, 1 (2004), ISSN 0031-9007.
- [26] A. Myerson, D. J. Szwer, S. C. Webster, D. T. C. Allcock, M. J. Curtis, G. Imreh, J. A. Sherman, D. N. Stacey, A. M. Steane, and D. M. Lucas, *Physical Review Letters* **100**, 200502 (2008), ISSN 0031-9007.
- [27] D. J. Wineland, personal communication.

## ACKNOWLEDGEMENTS

This work was supported by the EPSRC “Networked Quantum Information Technology” Hub and the U.S. Army Research Office (contract W911NF-14-1-0217).